Journal of Mechanical Engineering Research and Developments
ISSN: 1024-1752
Website: http://www.jmerd.org
Vol. 39, No. 3, 2016, pp. 633-639

Influence of Number and Arrange of Teeth on Performance of Labyrinth Seal

T. L. Jiang[†‡*], Z. M. Xu[‡], L. H. Cao[‡], W. Xu[‡], & Y. Li[‡]

[†]College of Energy and Mechanical Engineering, North China Electric Power University, Beijing 102206, China,
*Email: jiangtieliu@163.com

[‡]College of Energy and Power Engineering, Northeast Dianli University, Jilin 132012, China

ABSTRACT: In this paper, the SIMPLE methods and the RNG k-ε turbulence model are employed to investigate the effects of seal number and arrangement of teeth on the discharge behavior of a typical labyrinth seal. The results show that the flow field vortex system structure in the sealed chamber of the labyrinth seal changes with the variation of the seal number when the length of labyrinth seal section is constant. With the increase of the seal number, the vortex becomes complex, while the seal effect becomes better. When the seal number is same and the length of labyrinth seal section is fixed, the structure with higher teeth in the front and lower teeth in the back should be applied in order to reduce the labyrinth packing gas leakage.

KEYWORDS: Steam turbine; Labyrinth seal; Number of teeth; Arrange; Numerical simulation.

INTRODUCTION

As a sealing component of the steam turbine, the sealing property of gland sealing greatly influences the safe and economic operation of the steam turbine [1-3]. In continuous researches, it is found that: the fluid flows in a rather complicated manner inside the labyrinth seal, but the flow still accords with all the governing equations [4-6]. The inner flow filed as well as the pressure filed distribution of the seal cavity is obtained through numerical simulation, which is also the inevitable way to study the sealing property of gland sealing [7-10]. Researches show that the gland sealing leakage amount is greatly influenced by the shape and thickness of gland sealing gears [11]. Moreover, the leakage property of labyrinth seal is also influenced by sealing clearance, pressure ratio and rotation speed [12]. The numerical investigation method is used in the paper to mainly analyze the influence of gland sealing gear number and arrangement on its sealing property. The paper is intended to find the law about how the structure parameters of the gland sealing influence the leakage property, laying theoretical foundations for the design and improvement of the gland sealing.

CALCULATION MODEL AND NUMERICAL METHOD

Modeling and Meshing

The changes about inner flow filed and leakage amount of the gland sealing are studied in the paper when the gland sealing gear number gradually increases at the fixed length of the gland sealing [13,14]. For the stepped labyrinth gland, the increase of the gland gear number requires adjusting the clearance between stub gears and high gears of the gland sealing when the length of the gland sealing is fixed. Therefore, the paper studies five kinds of gland sealing structures including the gear number at 5,6,7,9 and 11 respectively. The diagram of the gland sealing structure is shown in Figure 1, where a represents the distance from the gear behind two stub gears of the gland sealing to the adjacent high gear, b represents the distance from the high gear to the gear behind the stub gear. For the gland sealing structure with different gear numbers and fixed length, a and b differ in value. The cavity spacing for five kinds of structures is shown in Table 1. Figure 2 shows the structural arrangement of the gland sealing about five kinds of gear numbers above.

To save the calculation time, the calculation arc of angle is used to analyze the inner flow filed of the whole gland sealing and the periodic boundary condition is adopted on two truncation surfaces of the arc without considering the eccentricity effect of the axis. The Gambit software is used for the three-dimensional geometric modeling of the calculation model. Meanwhile, the structural grid is adopted with encryption in near walls. The structured grid of the local computational domain is shown in Figure 3. The gridding number of the arc is determined between 330,000 and 410,000 after comparing the simulation results of different grids.

DOI: 10.7508/jmerd.2016.03.004

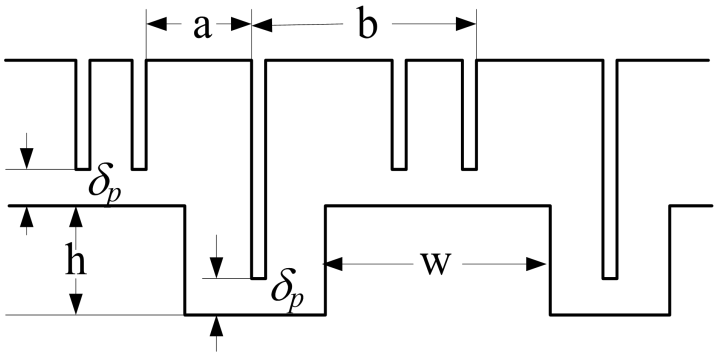

Figure 1. Diagram of gland sealing structure.

Table 1. Cavity structure parameters corresponding to different gland gear numbers.

zp	5	6	7	9	11
a (mm)	18	12	9	7	5.5
b (mm)	18	13	10	8	6.5

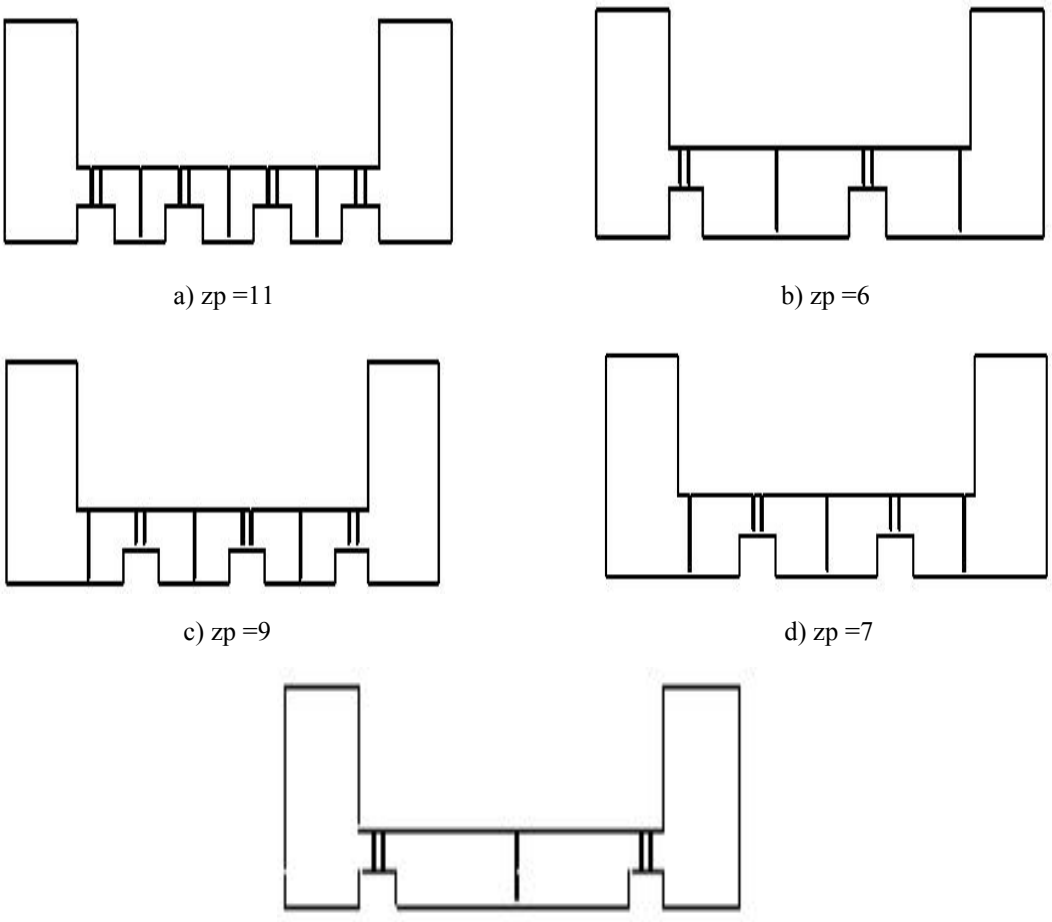

a) zp =11 b) zp =6

c) zp =9 d) zp =7

e） zp =5

Figure 2. Diagram of gland sealing structure arrangement.

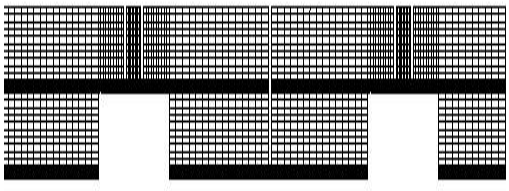

Figure 3. Structured grid of local computational domain.

Governing Equation

The general governing equation of the steady-state three dimensional hydrodynamics in the computational domain is described as follows:

$$\mathrm{div}(\rho u\phi) = \mathrm{div}(\Gamma_\phi \mathrm{grad}\phi) + \mathrm{S}_\phi \tag{1}$$

Where, ϕ is generic variable, u is speed, ρ is fluid density, Γ_ϕ is generalized diffusion coefficient, and S_ϕ is generalized source item.

The RNG $k-\varepsilon$ turbulence model, the turbulence viscosity of which is corrected, is used to consider the rotation of the average flow. The discrete control equation of the finite volume method is used with the help of the commercial computer software Fluent. Meanwhile, two-order upstream is used to solve the flow item, and first-order upstream to solve the diffusion item. Finally, the SIMPLE algorithm is used to solve the pressure-speed coupling.

Fluid Properties and Boundary Conditions

Fluid is defined as the steady-state three dimensional compressible flows, and fluid is calculated as high temperature and high pressure superheated water vapor. The Sutherland three-coefficient law is used to calculate viscosity changes. The boundaries of pressure inlet and pressure outlet are used in the computational domain, where the inlet is given the total pressure and temperature: with temperature at 414 3K and pressure at 0.87Mpa. Pressure is defined as the ratio of inlet pressure and outlet pressure. The residual error solution is controlled at 10-6. Heat insulation and non-slipping conditions are used on rotor walls with rotor speed expressed in n (r/min). Moreover, the standard wall function is used to solve the flow problem of near walls and the roughness is the rotor surface value.

RESULTS AND ANALYSIS

Influence of Gland Gear Number on Inner Flow Field

Vapor flows into the gland sealing from the pressure inlet on the left side and the flow is repeatable in each gland sealing, so the isomorph cavity between two stub gears is cut out for study in each gland arrangement. The cross sections of labyrinth models (five kinds of gear number) are enlarged to study the influence of vortex size and shape on sealing properties. Figure 4 shows the flow trajectory of vapor in the seal cavity. It can be seen that the gland sealing gear produces the vortex flow inside the gland sealing cavity. It is the inner vortex of the gland sealing gear that transforms the kinetic energy of vapor into the thermal energy, which reduces the flow speed of vapor and realizes the sealing function. The sealing effect depends on the throttling process of the labyrinth sealing clearance and the dissipation process of the kinetic energy inside gland sealing cavity.

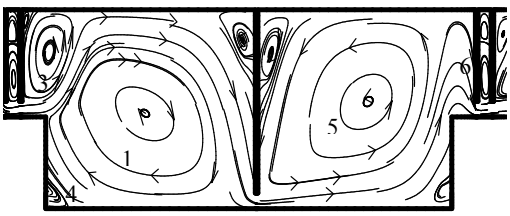

a) z_p =11

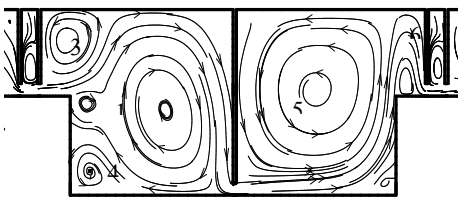

b) z_p =9

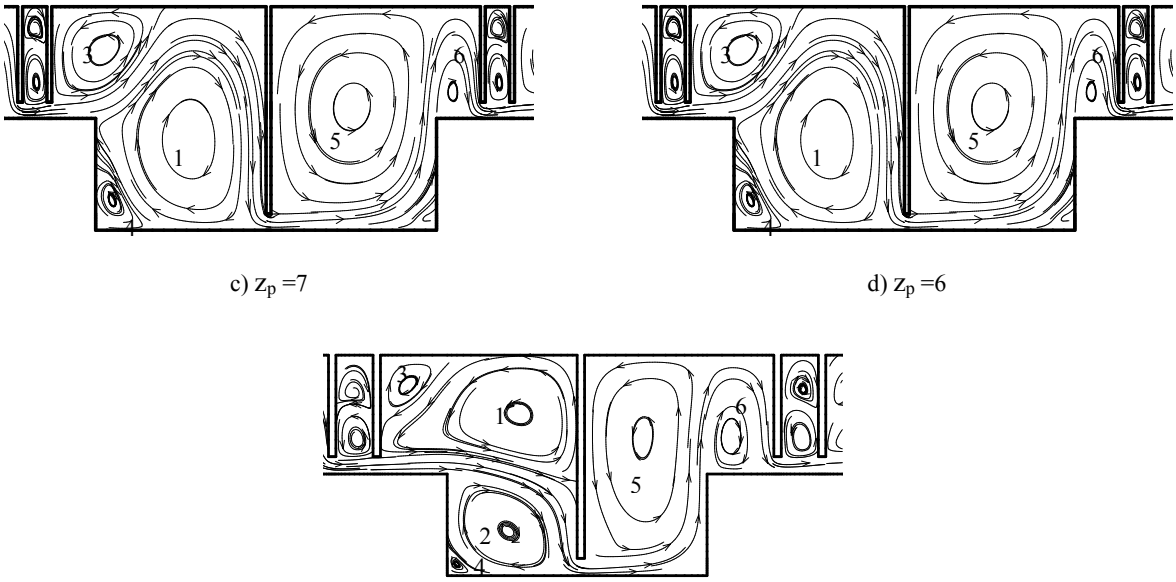

c) z_p =7

d) z_p =6

e) z_p =5

Figure 4. Motion pattern of cross sections for gland sealing with different gears.

It can be seen in Figure 4 that vapor first produces the jet flow from the throttling clearance and then impacts the incident flow wall of the high gland gear. The impacted jet flow is divided into three strands: the first strand directly flows to next gear clearance, while the other two strands are located on both sides of the first strand. The large left-rotation vortex above is named 1# vortex, while the right-rotation vortex formed below is named 2# vortex. The right cavity of the boss has more space, so 1# vortex is larger than 2# vortex. Meanwhile, the small right-rotation vortex is formed and named 3# vortex at the upper right corner when the fall-out of the 1# large vortex above the jet flow impacts the reverse flow of the stub gear. Similarly, the small left-rotation vortex is also formed at the lower right corner of the reverse flow and name 4# vortex.

After the cavity pressure is recovered, vapor flows to the cavity formed by the shoulder and the stub gear of incident flow through the narrow clearance of high gear. Through the depressurization of the gland sealing gear, the inflated vapor impacts the incident flow surface of the shoulder. After the airflow impact, a relatively large left-rotation vortex is formed between the reverse flow surface of the high gear and the boss and is named 5# vortex. The rest part of vapor continues to rise until it impacts the upper cavity wall, forming the small right-rotation vortex, which is named 6# vortex. The clearance flow flows to the cavity formed by two small stub gears when passing the stub gear above the boss, forming two small vortexes of opposite directions. The flow process above is constantly repeated by vapor in the cavity, causing the kinetic energy contained in the clearance jet flow to disappear because of internal friction. When equations z_p =11 and z_p =9 satisfy, it can be seen through analyzing the intercavity vortex that: some vapor of the clearance jet flow directly flows to next clearance without forming vortex when vapor passes the stub gear. Therefore, the enlarged clearance inevitably increases the leakage flow and weakens sealing properties. For the gland sealing structure with relatively fewer gears (7, 6 and 5), the vortex system is also different. With the decrease of gears, the value of sizes a and b for the structure of gland sealing cavity increases, and the cavity space also increases. The formed jet flow first impacts the upper wall of the cavity rather than the wall of the high gear incident flow in the large space when vapor passes the throttling orifice. It makes the directions of vortexes opposite to those formed by multi-gear structures, namely the direction of 1# vortex is right rotating, while 3# vortex is left rotating. However, the structures of 5# and 6# vortexes behind the reverse flow surface of the high gear are basically the same when equations zp =7 and zp =6 satisfy. Only the tiny vortex is formed at the lower left corner for the incident flow surface of the boss.

As gears constantly decrease in number, the size of the cavity keeps increasing. When the equation z_p =7 satisfies, it can be seen through comparing a) and c) in Figure 4 that: 1# vortex forms and develops more fully compared with the situation when the equation zp =11satisfies, occupying most of the cavity and causing 2# vortex to disappear. When the equation z_p =6 satisfies, both the cavity and the scope of 1# vortex enlarges more than z_p=7. Moreover, the backflow of large vortexes also intensifies. After the back flow drops out, it impacts the reverse flow surface of the

boss, forming the small left-rotation vortex at the downside reverse flow, while the rest backflow impacts the clearance flow, forming the small right-rotation vortex parallel to the boss in Figure d).

When z_p =5, the number of gears is relatively small, lengthening 1# and 5# vortexes, but the formation mechanism and the structure are basically the same as those of z_p =7. The difference lies in that: the jet flow impacts the cavity wall in a forward position with the increase of the sealing cavity, causing the decrease of 3# vortex. Moreover, the vortex structure is uneven with the intensified drop-out because 1# and 5# vortexes are long and narrow, thus forming the small vortex above both sides of high gears. Through analyzing and comparing the vortex system structures of the flow filed at fixed gland sealing length and different gear numbers, it is found that the relatively large gear clearance, namely the cavity large enough, can produce the strong dissipation vortex and the kinetic energy of vapor can be fully transformed into thermal energy when the number of gears is relatively small. Because of the short throttling process and the large throttling pressure drop every time, vapor moves at a relatively quick speed between gland clearances, causing much leakage and poor sealing effects. The number of cavities also increases with the increase of gear numbers, but the cavity can still form relatively strong vortexes and dissipate the vapor energy into thermal energy. Meanwhile, the increase of throttling processes reduces the throttling pressure drop every time, so the leakage reduces with relatively good sealing effects. Moreover, very little airflow enters the cavity between stub gears when vapor flows past the stub gear clearance, so the sealing function does not work very well.

Analysis of the Influence of Gland Sealing Gear Arrangement on Flow Field

To further study the structure and number of vortexes formed in the sealing cavity when the structures of different gland sealing arrangements are different, the flow pattern of Z=0 surface for two kinds of different gear numbers (z_p =6 and zp =9) is given as shown in Figure 5. The arrangement feature of z_p =6 and zp =9 is that the first gland sealing gear structure differs from the last one. By comparing a) and b) in Figure 5, it can be seen that: except the first cavity in two arrangements, the vortex system structures formed by the leakage are basically the same when z_p =9. However, slight changes are found in the vortex systems of c) and d) when z_p =6. The difference lies in that small vortexes are formed on the right side for the reverse flow surface of the boss in Figure c), which is parallel to the boss. The formation mechanism of vortexes has been described above, so it will not be repeated here.

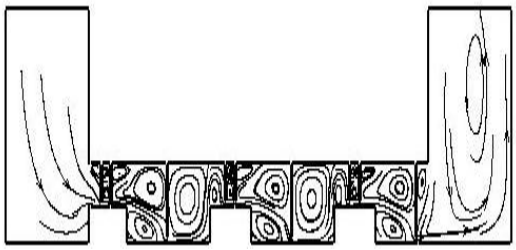

a) z_p =9, arrangement of front stub gear and back high gear

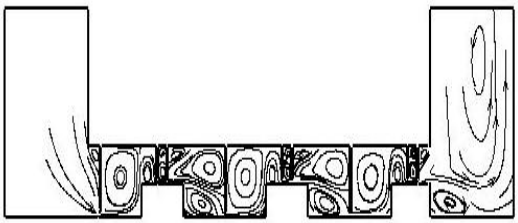

b) z_p =9, arrangement of front high gear and back stub gear

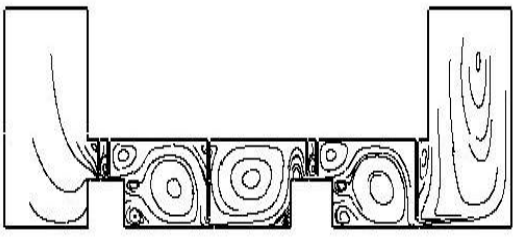

c) z_p =6, arrangement of front stub gear and back high gear

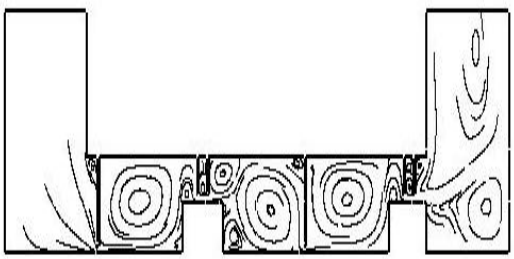

d) z_p =6, arrangement of front high gear and back stub gear

Figure 5. Two-dimensional flow pattern of the cavity with different gland sealing gear arrangements.

In addition, certain changes are found in the leakage amount of the gland sealing with two kinds of gear shapes as shown in Table 2. With two kinds of gear numbers, the alternate arrangement of high-stub gears produces slightly less leakage than that of stub-high gear gears, which is closely associated with the vortex structure and the pressure cloud chart with different arrangements. Take z_p =6 structure for example, Figure 6 shows the cloud chart of the pressure distribution in the gland sealing cavity of Z=0mm surface when different arrangements are given. For the gland sealing structure with the same gear number, the calculation can be realized only by changing inlet and outlet conditions in the numerical calculation with the workload reduced, so the pressure inlet is placed on the right side of b) in Figure 6, which is opposite to Figure a). By comparing the pressure contour lines that enter the first large-size gland sealing cavity from a) and b) in Figure 6, it can be seen that: the pressure value of the alternate high-stub gear arrangement is obviously larger than that of stub-high gear arrangement, making the differential pressure before and after the first gland sealing gear relatively large and increasing the leakage amount of the gland sealing. Therefore, the structural arrangement of high-stub gears should be adopted to reduce the leakage amount of the gland sealing when the number of gears is the same and the length of the gland sealing is fixed [15].

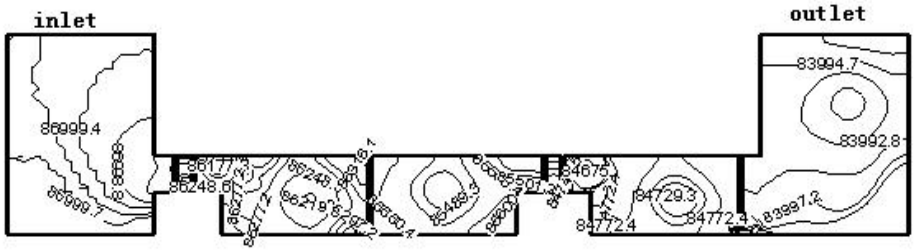

a) Stub-high gear arrangement

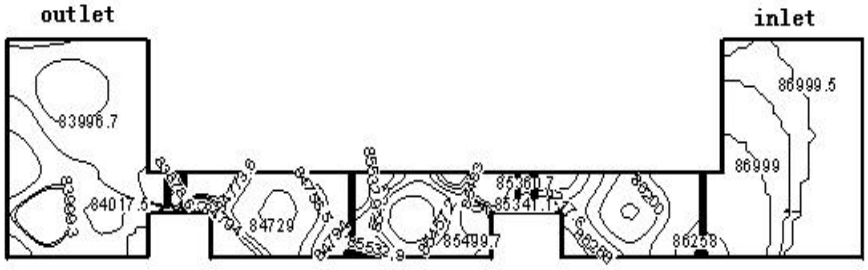

b) High-stub gear arrangement

Figure 6. Pressure cloud chart of different gland sealing gear arrangements when Zp=6.

In addition, certain changes are found in the leakage amount of the gland sealing with two kinds of gear shapes as shown in Table 2. With two kinds of gear numbers, the alternate arrangement of high-stub gears produces slightly less leakage than that of stub-high gear gears, which is closely associated with the vortex structure and the pressure cloud chart with different arrangements. Take z_p =6 structure for example, Figure 6 shows the cloud chart of the pressure distribution in the gland sealing cavity of Z=0mm surface when different arrangements are given. For the gland sealing structure with the same gear number, the calculation can be realized only by changing inlet and outlet conditions in the numerical calculation with the workload reduced, so the pressure inlet is placed on the right side of b) in Figure 6, which is opposite to Figure a). By comparing the pressure contour lines that enter the first large-size gland sealing cavity from a) and b) in Figure 6, it can be seen that: the pressure value of the alternate high-stub gear arrangement is obviously larger than that of stub-high gear arrangement, making the differential pressure before and after the first gland sealing gear relatively large and increasing the leakage amount of the gland sealing. Therefore, the structural arrangement of high-stub gears should be adopted to reduce the leakage amount of the gland sealing when the number of gears is the same and the length of the gland sealing is fixed.

Table 2. Leakage amounts of different gland sealing arrangements (kg/h).

Gear number of gland sealing	High-stub gear arrangement	Stub-high gear arrangement
z_p =9	1.304	1.323
z_p =6	1.647	1.670

CONCLUSIONS

(1) The flow-field vortex system structure is different when the length of gland sealing section is fixed and the number of gears is different. The larger the number of gears is, the more complicated vortexes will be.

(2) When the number of gland sealing gears is small, vapor flows relatively quickly between gear clearances because of the large throttling pressure drop every time, thus causing much leakage and poor sealing effects. Conversely, the increase of gears can still form relatively stronger vortexes in the sealing cavity and reduces the throttling pressure drop, so it produces less leakage and good sealing effects.

(3) The stub-high gear structural arrangement should be adopted to reduce the gland sealing leakage when the number of gears is the same and the length of gland sealing is fixed.

ACKNOWLEDGEMENTS

This research is supported by National Natural Science Foundation of China (NSFC) (51376041).

REFERENCES

[1] R. E. Chupp, R. C. Hendricks, and S. B. Lattime, “Sealing in turbo machinery”, *J Propul Power*, vol. 22, no. 2, pp. 313-349, 2006.

[2] H. Cai, B. Zhu, and H. D. Jiang, “Numerical study about the main influence of seal leakage flow on turbine blade path”, *J Eng Thermophys-Rus*, vol. 22, no. 3, pp. 290-293, 2001.

[3] X. K. Tian and R. Y. Zhao, “Energy network flow model and optimization based on energy hub for big harbor industrial park”, *Journal of Coastal Research: Special Issue* 73, pp. 298-303.

[4] Q. Cui, Z. H. Zhang, and Y. Zhou, “Experimental study of turbine gland leakage”, *Thermal Turbine*, vol 39, no.1, pp. 26-30, 2010.

[5] Y. J. Zhu, R. Dai, and Q. Y. Sai, “Function and design of splitter blades in low-speed compressor cascade”, *J Eng Thermophys-Rus*, vol 35, no. 12, pp. 2402-2405, 2014.

[6] Q. Cui, Z. H. Zhang, and W. K. Liu, “Test research of the leakage performance in steam seal”, in *ASME 2011 Power Conference Collocated with Jsme Icope*, 2011, pp. 727-732.

[7] L. Y. Jiang, W. K. Liu, and Z. H. Zhang, “Comparing sealing properties of stage gears, honeycomb gland sealing and cellular-type damping gland sealing”, *Journal of Power Engineering*, vol. 32, no. 7, pp. 508-512, 2012.

[8] L. H. Cao, P. F. Hu, and W. Xu, “Numerical simulation of inner flow filed for dynamic-static gland sealing”, *Chemical Machinery*, vol. 37, no. 5, pp. 617-621, 2010.

[9] Z. H. Zhang, F. Fan, K. X. Wang, and B. Franciosa, “Analysis on seismic performance of centrically braced steel frame”, *Journal of Mechanical Engineering Research and Developments*, vol. 39, no. 2, pp. 308-314, 2016.

[10] Z. X. Luan, Y. Li, and Y. G. Xue, “Numerical study on secondary flow losses of stationary turbine cascade”, *Journal of Northeast Dianli University*, vol. 32, no. 2, pp. 43-47, 2012.

[11] J. Ahmed, M. Gamal, and M. John, “Labyrinth seal leakage tests: Gear profile, gear thickness, and eccentricity effects”, *ASME Journal of Engineering for Gas Turbines and Power*, vol. 130, pp. 012510.1-012510.11, 2008.

[12] Z. G. Li, J. Li, and Z. P. Feng, “Study on influence factors of labyrinth sealing leakage properties”, *Journal of Xi'an Jiaotong University*, vol. 44, no.3, pp.16-22, 2010.

[13] J. Zhang and H. Kazerooni, “Consideration on the building of urban landscape sports culture”, *Journal of Mechanical Engineering Research and Developments*, vol. 39, no. 1, pp. 83-87, 2016.

[14] Z. J. Hou, Z. Q. Lu, J. Z. Liang, C. Chen, and Y. Xu, “A healthy monitor system for fall and balance detection of elderly”, vol. 39, no. 2, pp. 364-372, 2016.

[15] H. Hui, Z. L. Liu, and H. B. Liu, “The Coordination Analysis of the Energy Consumption, Economy Growth, and Environment Protection in China”, *EBM 2010: International Conference on Engineering and Business Management*, vol. 1-8, pp. 5596-5599.